

# Electronic structure and possible pseudogap behavior in iron based superconductors

*E. Z. Kuchinskii M. V. Sadovskii<sup>1)</sup>*

*Institute for Electrophysics, Russian Academy of Sciences, Ural Branch, 620016 Ekaterinburg, Russia*

Submitted \*

Starting from the simplified analytic model of electronic spectrum of iron - pnictogen (chalcogen) high - temperature superconductors close to the Fermi level, we discuss the influence of antiferromagnetism (AFM) scattering both for stoichiometric case and the region of possible short - range order AFM fluctuations in doped compounds. Qualitative picture of the evolution of electronic spectrum and Fermi surfaces (FS) for different dopings is presented, with the aim of comparison with existing and future ARPES experiments. Both electron and hole dopings are considered and possible pseudogap behavior connected with partial FS “destruction” is demonstrated, explaining some recent experiments.

PACS: 71.10.Hf, 71.18.+y, 74.25.Jb, 74.70.-b, 74.72.-h

Recent discovery of the new class of iron based high-temperature superconductors [1] stimulated intensive of experimental and theoretical efforts to understand its properties (see for the review Refs. [2, 3]). Despite already the immense progress in understanding of these systems, the nature of superconducting pairing and anomalies in the normal state are still under debate.

Clarification of the structure of electronic spectrum of new superconductors is crucial for explanation of their physical properties. Accordingly, since the first days, different groups have started the detailed band - structure calculations for all classes of these compounds, based primarily on different realizations of general LDA approach. These calculations were primarily performed for paramagnetic tetragonal FeAs 1111 systems [4, 5, 6, 7], for 122 [8, 9, 10], for 111 [10, 11, 12] and  $\alpha$ -FeSe [13], followed by many similar works by other authors. In fact, all these calculations demonstrated almost universal LDA band structure in relatively narrow energy interval ( $\pm 0.1eV$ ) around the Fermi level, which is of relevance to superconductivity [2].

In this energy interval the electronic spectrum can be modelled analytically as follows. Three “hole-like” branches of the spectrum crossing the Fermi level near the  $\Gamma$  point in the Brillouin zone (cf. Fig.1a) can be taken isotropic and modelled by quadratic dispersion:

$$\varepsilon_i(\mathbf{p}) = \varepsilon_i - \frac{p^2}{2m_i} \quad (1)$$

where  $m_i$ ,  $\varepsilon_i$  ( $i = 1, 2, 3$ ) can be easily determined from LDA calculations (e.g. for 122 system from the results of Ref. [8]).

Two “electron-like” branches of the spectrum crossing the Fermi level near  $M(\pi, \pi)$  point of the reduced Brillouin zone are anisotropic and produce two elliptic isoenergetic crosssections at the Fermi level (cf. Fig.1b), one of which is extended in the direction  $M\Gamma$ , with the second one extended in the orthogonal direction. Let us count the momentum from the  $M$  point (i.e. replace  $\mathbf{p} - \mathbf{Q} \rightarrow \mathbf{p}$ ) and take one momentum  $\mathbf{p}$  axis along  $M\Gamma$  direction and other orthogonal to it (Fig.1b). The relevant momentum projections  $p_1$  and  $p_2$  are connected with the usual  $x$ ,  $y$  projections as  $p_1 = \frac{p_y + p_x}{\sqrt{2}}$ ,  $p_2 = \frac{p_y - p_x}{\sqrt{2}}$ . Consider one of the ellipses, e.g. those extended along the direction orthogonal to  $M\Gamma$  direction. Electron dispersion along  $M\Gamma$  can be modelled by quadratic law  $\varepsilon_{p1}(p) = \frac{p^2}{2m_4} - \varepsilon_4$ . Dispersion along the orthogonal (to  $M\Gamma$ ) direction is determined by higher (in energy) branch of the spectrum, originating from the hybridization of two “bare” dispersions (cf. Fig. 1a), which we also assume quadratic. Then, neglecting the small hybridization gap, we obtain  $\varepsilon_{p2}(p) = \text{Max}(-\frac{p^2}{2m_0} - \varepsilon_4; \frac{p^2}{2m_5} - \varepsilon_5)$  Parameters  $m_4, \varepsilon_4, m_5, \varepsilon_5, m_0$  can be taken from LDA data. Thus, for anisotropic “electron-like” spectrum we can use the following model:

$$\varepsilon_4(\mathbf{p}) = \cos^2(\phi)\varepsilon_{p1}(p) + \sin^2(\phi)\varepsilon_{p2}(p) \quad (2)$$

where  $p^2 = p_1^2 + p_2^2$ , and  $\phi$  is the polar angle with respect to  $p_1$  axis. This model guarantees correct energy crosssections in direction  $M\Gamma$  and orthogonal it, as well as isotropy of the spectrum in case of  $\varepsilon_{p1}(p) = \varepsilon_{p2}(p)$ .

<sup>1)</sup>E-mail: sadovskii@iep.uran.ru

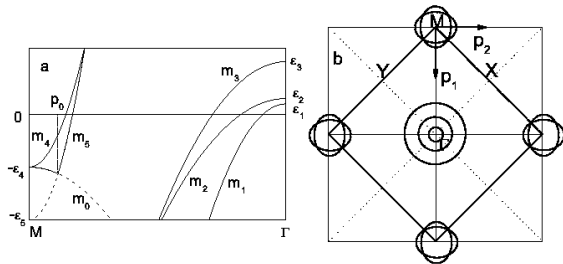


Fig.1. Qualitative picture from of the band structure in  $M\Gamma$  direction in the reduced Brillouin zone (a) and the relevant Fermi surfaces (b).

Energy dispersion for the second “electron-like” band  $\varepsilon_5(\mathbf{p})$  is also given by Eq. (2) with the obvious substitution  $\phi \rightarrow \frac{\pi}{2} + \phi$ . Finally, we describe the “electron-like” bands in our model as:

$$\varepsilon_4(\mathbf{p}) = \begin{cases} \frac{p_1^2}{2m_4} - \frac{p_2^2}{2m_0} - \varepsilon_4 & \text{for } p^2 = p_1^2 + p_2^2 < p_0^2 \\ \frac{p_1^2}{2m_4} + \frac{p_2^2}{2m_5} - \frac{p_1^2}{p^2} \varepsilon_4 - \frac{p_2^2}{p^2} \varepsilon_5 & \text{for } p^2 > p_0^2 \end{cases} \quad (3)$$

where  $p_0^2 = 2(\varepsilon_5 - \varepsilon_4)/(\frac{1}{m_5} + \frac{1}{m_0})$  is the square of the momentum at the crossing of two “bare” hybridizing bands.

The qualitative picture of electronic spectrum and Fermi surfaces is shown in Fig. 1. Essentially this kind of electronic spectra and Fermi surfaces in new superconductors were qualitatively confirmed by angle resolved photoemission spectroscopy (ARPES), starting with the early works [14, 15, 16, 17, 18, 19, 20, 21], followed by many further studies by the same and other authors. Most of these experiments were performed on single crystals of 122 systems, while for other compounds good quality single crystals are up to now just unavailable. Though in qualitative agreement with the results of LDA calculations, these experiments show rather different results concerning finer details, such as the precise number of “hole-like” FS cylinders around the  $\Gamma$  point, as well as the topology of “electron-like” cylinders around the  $M$  – point.

In general LDA calculations underestimate the role of electronic correlations. ARPES experiments show that these systems apparently belong to the class of intermediately correlated systems, with correlation induced band narrowing by the factor of two [16]. This is confirmed by some of LDA+DMFT calculations [22], though theoretical situation here remains rather controversial. In the following we take correlations into

$$\frac{i}{G_{ij}^n} = \frac{i}{G_{0i}^n \delta_{ij}} + \frac{i}{G_{0i}^n} \frac{\Delta^2 s(n+1)}{G_{lm}^{n+1}} \frac{i}{G_{lj}^n}$$

Fig.2. Recurrence “Dyson equation” for the Green’s function.

account by simple rescaling of the energy by the factor of two as compared with LDA [16].

Undoped FeAs compounds are antiferromagnetically ordered with AFM vector  $\mathbf{Q} = (0, \pi)$  in extended Brillouin zone, corresponding to  $\mathbf{Q} = (\pi, \pi)$  in the reduced zone [2, 3]. Electron or hole doping suppresses AFM ordering and induces superconductivity, similar to the well known situation in cuprates. Recent neutron scattering experiments [23, 24] clearly show that in the substantial part of the phase diagram of FeAs systems in normal paramagnetic state rather strong fluctuations of AFM short-range order persist, as predicted e.g. by the model of “nearly antiferromagnetic Fermi liquid” [25, 26, 27]. These fluctuations can, in principle, induce the pseudogap behavior in electronic spectrum, similar to that observed in cuprates [28].

Effective interaction of electrons with AFM spin fluctuations is determined in this model by dynamic spin susceptibility characterized by the maximum at scattering vectors close to AFM vector  $\mathbf{Q} = (\pi, \pi)$ , which we assume here to be the same for electron from different bands and for interband scattering. Limiting ourselves to high enough temperatures we can neglect the dynamics of AFM fluctuations and consider them Gaussian [28]. The Green’s function for electrons moving in the “quenched” Gaussian random field of these fluctuations can be represented by recurrence “Dyson equation” shown in Fig.2, which is the direct multiple bands generalization of the summation procedure, proposed and actively used in Refs. [29, 30, 31, 32], taking into account *all* Feynman diagrams for electron scattering in such random field.

Analytically, this “Dyson equation” can be written as:

$$G_{ij}^n = G_{0i}^n \delta_{ij} + G_{0i}^n \Delta^2 s(n+1) \sum_{km} G_{km}^{n+1} \sum_l G_{lj}^n \quad (4)$$

where  $i, j$  represent band indices,  $\Delta$  characterizes the AFM pseudogap width (of the order of AFM band splitting),

$$G_{0i}^n(E\mathbf{p}) = \frac{1}{E - \varepsilon_i^n(\mathbf{p}) + i\nu v_i^n \kappa} \quad (5)$$

$\kappa = \xi^{-1}$  is an inverse correlation length of AFM short-range order fluctuations,  $\varepsilon_i^n(\mathbf{p}) = \varepsilon_i(\mathbf{p} + \mathbf{Q})$  and  $v_i^n = |v_i^x(\mathbf{p} + \mathbf{Q})| + |v_i^y(\mathbf{p} + \mathbf{Q})|$  for odd  $n$ , while  $\varepsilon_i^n(\mathbf{p}) = \varepsilon_i(\mathbf{p})$

and  $v_i^n = |v_i^x(\mathbf{p})| + |v_i^y(\mathbf{p})|$  for even  $n$ . Velocity projections  $v_i^x(\mathbf{p})$  and  $v_i^y(\mathbf{p})$  are determined by the momentum derivatives of electronic dispersion in the  $i$ -th band  $\varepsilon_i(\mathbf{p})$ . Combinatorial factor  $s(n)$  for the case of Heisenberg AFM fluctuations (spin-fermion model of Ref. [31]) is given by:

$$s(n) = \begin{cases} \frac{n+2}{3} & \text{for odd } n \\ \frac{n}{3} & \text{for even } n. \end{cases} \quad (6)$$

The physical Green's function corresponds to  $n = 0$ . Then, after some simple manipulations we may show that

$$G_{ij}(E\mathbf{p}) = G_{0i}^0(E\mathbf{p})\delta_{ij} + \frac{G_{0i}^0(E\mathbf{p})G_{0j}^0(E\mathbf{p})\Sigma(E\mathbf{p})}{1 - G_0^0(E\mathbf{p})\Sigma(E\mathbf{p})} \quad (7)$$

where the physical self-energy

$$\Sigma(E\mathbf{p}) = \Sigma^{n=1}(E\mathbf{p}) \quad (8)$$

is determined from the recurrence procedure (continued fraction representation):

$$\Sigma^n(E\mathbf{p}) = \frac{\Delta^2 s(n)}{(G_0^n(E\mathbf{p}))^{-1} - \Sigma^{n+1}(E\mathbf{p})} \quad (9)$$

where  $G_0^n(E\mathbf{p}) = \sum_j G_{0j}^n(E\mathbf{p})$ . As a byproduct of these general equations we can easily analyze the electronic spectrum in the case of AFM long-range order, truncating the continuous fraction in Eq. (9) at  $n = 1$  and taking the limit of  $\kappa \rightarrow 0$ . The spectral density and density of states are obviously given by:

$$A(E\mathbf{p}) = -\frac{1}{\pi} \text{Im} S p G_{ii}^R(E\mathbf{p}); \quad N(E) = \sum_{\mathbf{p}} A(E, \mathbf{p}) \quad (10)$$

We performed calculations for a variety of parameters of the model, using for the spectrum LDA data for 122 from Ref [8], scaled by factor of two to account for correlations. Below we present results for  $\Delta = 50$  meV, which is in rough agreement with the estimates of AFM band splitting from ARPES data [33, 34] and neutron scattering [35] (varying in the interval 50-100 meV), correlation length of AFM fluctuations  $\xi = 10a$  ( $a$  - lattice spacing), also in rough agreement with neutron scattering data [23, 24]. In the following, all momenta are given in units of inverse lattice spacing, energies in eV. To make the results comparable with ARPES experiments we have also introduced effective widening to simulate finite energy resolution of ARPES replacing  $E \rightarrow E + i\gamma$  and taking  $\gamma = 10$  meV (corresponding to best ARPES resolution).

In Fig. 3 we show ‘‘ARPES’’ energy bands of 122 system, revealed by the maps of spectral density, along

main symmetry directions, starting from the case of normal (paramagnetic) LDA bands, via AFM long-range ordered state, to ‘‘pseudogapped’’ state, characterized by electrons scattered by short-range ordered AFM fluctuations – AFM band splittings transforming to pseudogaps due to AFM short-range order.

In Fig. 4 we show spectral density maps at the Fermi level for different dopings – from slightly electron doped, via undoped, to hole underdoped and optimally hole doped case. These maps essentially produce ‘‘ARPES’’ Fermi surfaces of 122 system at different dopings. In fact, the system always remains metallic in a sense that at every doping we observe ‘‘open’’ Fermi surfaces, though we also can see rather complicated series of Fermi surface transformations, with some cylinders being almost ‘‘destroyed’’ (damped) either by AFM long-range order, or by short-range order AFM fluctuations. Of these maps, we identify the last one in the third row (4c) as corresponding more or less to optimally hole doped case in satisfactory agreement with ARPES data e.g. from Refs. [16, 18, 20, 36], while the third one in the same row (3c) apparently well corresponds to the hole underdoped case studied in Ref. [36], demonstrating the inner hole cylinder rather damped by pseudogap fluctuations with characteristic wave vector of the order of AFM vector  $\mathbf{Q}$ . Significant pseudogap forms in the (partial) density of states on precisely this cylinder, in agreement with Ref. [36]. In general, the available ARPES data suffer from rather bad resolution, so that pseudogap fluctuations can significantly complicate observation of all FS cylinders and much work is needed to reveal possible complicated picture of FS transformations, illustrated in Fig. 4. It should be taken into account that pictures shown in the second row (b) of Fig. 4 are sensible only within the part of the phase diagram with AFM long-range order, while the third row (c) applies to paramagnetic region, where superconductivity appears at lower temperatures.

Our calculations show, that the pseudogap forms only in (partial) densities of states, corresponding to those cylinders strongly affected by short-range AFM fluctuations, and this is not, in general, ‘‘pinned’’ at the Fermi level. Pseudogap in the total density of states is always rather weak, and the problem remains, whether it is sufficient to explain claims for the pseudogap behavior observed in some NMR experiments [2, 3].

This work is partly supported by RFBR grant 08-02-00021 and Programs of Fundamental Research of the Russian Academy of Sciences (RAS) ‘‘Quantum physics of condensed matter’’ (09-II-2-1009) and of the Physics Division of RAS ‘‘Strongly correlated electrons in solid states’’ (09-T-2-1011).

- 
1. Y. Kamihara, T. Watanabe, M. Hirano, H. Hosono. *J. Am. Chem. Soc.* **130**, 3296-3297 (2008)
  2. M.V. Sadovskii, *Uspekhi Fiz. Nauk* **178**, 1243 (2008); *Physics Uspekhi* **51**, No. 12 (2008); arXiv: 0812.0302
  3. K. Ishida, Y. Nakai, H. Hosono. *Journal of the Physical Society of Japan*, **78**, 062001 (2009)
  4. L. Boeri, O.V. Dolgov, A.A. Golubov. *Phys. Rev. Lett.* **101**, 026403 (2008)
  5. I.I. Mazin, D.J. Singh, M.D. Johannes, M.H. Du. *Phys. Rev. Lett.* **101**, 057003 (2008)
  6. G. Xu, W. Ming, Y. Yao, Xi Dai, S.-C. Zhang, Z. Fang. *Europhys. Lett.* **82**, 67002 (2008)
  7. I.A. Nekrasov, Z.V. Pchelkina, M.V. Sadovskii. *Pis'ma v ZhETF* **87**, 647 (2008); *JETP Letters* **87**, 620 (2008)
  8. I.A. Nekrasov, Z.V. Pchelkina, M.V. Sadovskii. *Pis'ma v ZhETF* **88**, 155 (2008); *JETP Letters* **88**, 144 (2008);
  9. I.R. Shein, A.L. Ivanovskii. *Pis'ma v ZhETF* **88**, 115 (2008)
  10. D.J. Singh. *Phys. Rev. B* **78**, 094511 (2008)
  11. I.A. Nekrasov, Z.V. Pchelkina, M.V. Sadovskii. *Pis'ma v ZhETF* **88**, 621 (2008); *JETP Letters* **88**, 543 (2008)
  12. I.R. Shein, A.L. Ivanovskii. *Pis'ma v ZhETF (JETP Letters)* **88**, 377 (2008)
  13. A. Subedi, L. Zhang, D.J. Singh, M.H. Du, *Phys. Rev.* **B78**, 134514 (2008)
  14. L.X. Yang, H.W. Ou, J.F. Zhao, Y. Zhang, D.W. Shen, B. Zhou, J. Wei, F. Chen, M. Xu, C. He, X.F. Wang, T. Wu, G. Wu, Y. Chen, X.H. Chen, Z.D. Wang, D.L. Feng, *Phys. Rev. Lett.* **102**, 107002 (2009)
  15. C. Liu, G.D. Samolyuk, Y. Lee, N. Ni, T. Kondo, A.F. Santander-Syro, S.L. Bud'ko, J.L. McChesney, E. Rotenberg, T. Valla, A.V. Fedorov, P.C. Canfield, B.N. Harmon, A. Kaminski, *Phys. Rev. Lett.* **101**, 177005 (2008)
  16. H. Liu, W. Zhang, L. Zhao, X. Jia, J. Meng, G. Liu, X. Dong, G.F. Chen, J.L. Luo, N.L. Wang, W. Lu, G. Wang, Y. Zhou, Y. Zhu, X. Wang, Z. Xu, C. Chen, X.J. Zhou, *Phys. Rev. B* **78**, 184514 (2008)
  17. L. Zhao, H. Liu, W. Zhang, J. Meng, X. Jia, G. Liu, X. Dong, G.F. Chen, J.L. Luo, N.L. Wang, W. Lu, G. Wang, Y. Zhou, Y. Zhu, X. Wang, Z. Zhao, Z. Xu, C. Chen, X.J. Zhou, *Chin. Phys. Lett.* **25**, 4402-4405(2008)
  18. H. Ding, P. Richard, K. Nakayama, T. Sugawara, T. Arakane, Y. Sekiba, A. Takayama, S. Souma, T. Sato, T. Takahashi, Z. Wang, X. Dai, Z. Fang, G.F. Chen, J.L. Luo, N.L. Wang. *Europhys. Lett.* **83**, 47001 (2008)
  19. V.B. Zabolotnyy, D.S. Inosov, D.V. Evtushinsky, A. Koitzsch, A.A. Kordyuk, J.T. Park, D. Haug, V. Hinkov, A.V. Boris, D.L. Sun, G.L. Sun, C.T. Lin, B. Keimer, M. Knupfer, B. Büchner, A. Varykhalov, R. Follath, S.V. Borisenko, *Nature* **457**, 569 (2009)
  20. D.V. Evtushinsky, D.S. Inosov, V.B. Zabolotnyy, A. Koitzsch, M. Knupfer, B. Büchner, G.L. Sun, V. Hinkov, A.V. Boris, C.T. Lin, B. Keimer, A. Varykhalov, A.A. Kordyuk, S.V. Borisenko, *Phys. Rev. B* **79**, 054517 (2009)
  21. T. Sato, K. Nakayama, Y. Sekiba, P. Richard, Y.-M. Xu, S. Souma, T. Takahashi, G.F. Chen, J.L. Luo, N.L. Wang, H. Ding, *Phys. Rev. Lett.* **103**, 047002 (2009)
  22. S.L. Skornyakov, A.V. Efremov, N.A. Skorikov, M.A. Korotin, Yu.A. Izyumov, V.I. Anisimov, A.V. Kozhevnikov, D. Vollhardt. *Phys. Rev.* **80**, 092501 (2009)
  23. D.S. Inosov, J.T. Park, P. Bourges, D.L. Sun, Y. Sidis, A. Schneidewind, K. Hradil, D. Haug, C.T. Lin, B. Keimer, V. Hinkov. *Nature Physics* **6**, 178 (2010)
  24. S.O. diallo, D.K. Pratt, R.M. Fernandes, W. Tian, J.L. Zaretsky, M. Lumsden, T.G. Perring, C.L. Broholm, N. Ni, S.L. Bud'ko, P.C. Canfield, H.-F. Li, D. Vaknin, A. Kreyssig, A.I. Goldman, R.J. McQueeney, arXiv:1001.2804
  25. T. Moriya. *Spin Fluctuations in Itinerant Electromagnetism*. Springer, 1985
  26. P. Monthoux, A. Balatsky, D. Pines. *Phys.Rev.* **B46**, 14803 (1992)
  27. P. Monthoux, D. Pines. *Phys.Rev.* **B47**, 6069 (1993); *Phys.Rev.* **B48**, 4261 (1994)
  28. M.V. Sadovskii, *Uspekhi Fiz. Nauk.* **171**, 539 (2001) [*Physics Uspekhi* **44**, 515 (2001)]; M.V. Sadovskii, in "Strings, branes, lattices, networks, pseudogaps and dust", Scientific World, Moscow, 2007, p. 357 (in Russian), English version: cond-mat/0408489
  29. M. V. Sadovskii, *Zh. Eksp. Teor. Fiz.* **77**, 2070(1979); [*Sov.Phys.-JETP* **50**, 989 (1979)]
  30. M.V. Sadovskii, *Diagrammatics*, Ch. 6, World Scientific, 2006
  31. J. Schmalian, D. Pines, B.Stojkovic, *Phys. Rev. B* **60**, 667 (1999).
  32. E. Z. Kuchinskii, M. V. Sadovskii, *Zh. Eksp. Teor. Fiz.* **115**, 1765 (1999) [*JETP* **88**, 347 (1999)].
  33. L.X. Yang, Y. Zhang, H.W. Ou, J.F. Zhao, D.W. Shen, B. Zhou, J. Wei, F. Chen, M. Xu, C. He, Y. Chen, Z.D. Wang, T. Wu, G. Wu, X.H. Chen, M. Arita, K. Shimada, M. Taniguchi, Z.Y. Lu, T. Xiang, D.L. Feng. *Phys. Rev. Lett.* **102**, 107002 (2009)
  34. Y. Zhang, J. Wei, H.W. Ou, J.F. Zhao, B. Zhou, F. Chen, M. Xu, C. He, G. Wu, H. Chen, M. Arita, K. Shimada, H. Namatame, M. Taniguchi, X.H. Chen, D.L. Feng. *Phys. Rev. Lett.* **102**, 127003 (2009)
  35. J. Knolle, I. Eremin, A.V. Chubukov, R. Moessner. *Phys. Rev.* **B81**, 140506 (2010)
  36. Y.-M. Xu, P. Richard, K. Nakayama, T. Kawahara, Y. Sekiba, T. Qian, M. Neupane, S. Souma, T. Sato, T. Takahashi, H. Luo, H.-H. Wen, G.-F. Chen, N.-L. Wang, Z. Wang, Z. Fang, X. Dai, H. Ding, arXiv:0905.4467

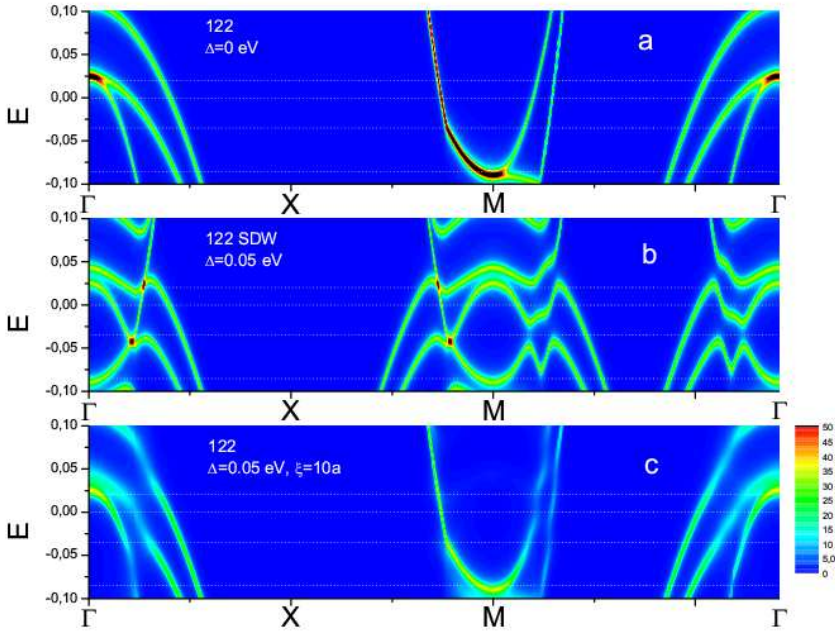


Fig.3. Energy bands. Upper panel (a) – “bare” (scaled LDA) bands in paramagnetic state in the absence of AFM fluctuations. Panel (b) – AFM long-range ordered state with  $\Delta = 0.05$  eV. Panel (c) – bands in the pseudogap state induced by AFM short-range order fluctuations with  $\xi = 10a$  and  $\Delta = 0.05$  eV. All bands are shown with finite “experimental” resolution  $\gamma = 0.01$  eV. Dotted lines show Fermi levels for different dopings used in our calculations of Fermi surfaces below.

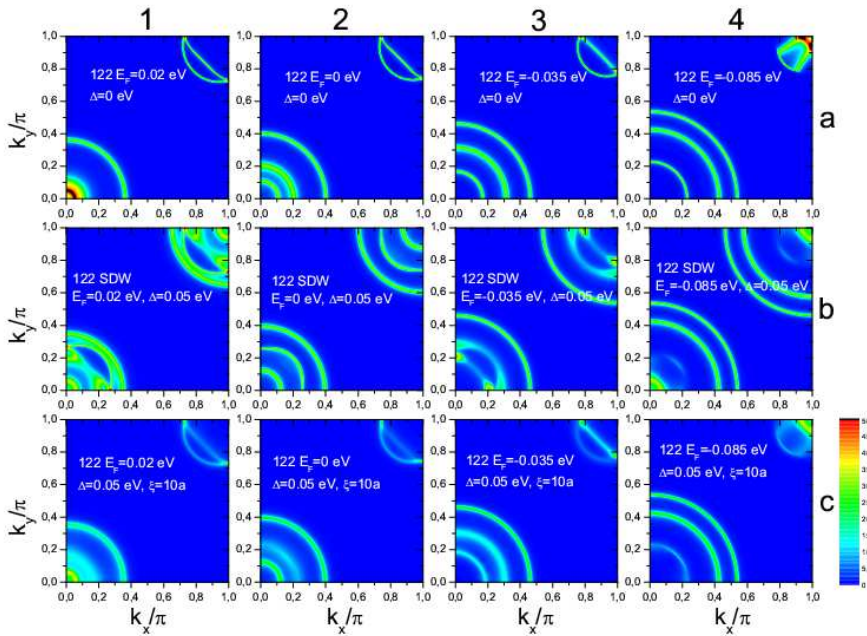


Fig.4. “ARPES” Fermi surfaces at different doping levels shown by dotted lines in Fig.3: Column 1 – electron doping with  $E_F = 0.02$  eV, 2 – undoped system with  $E_F = 0$ , 3 – hole doping with  $E_F = -0.035$  eV (hole underdoped system), 4 – optimal hole doping with  $E_F = -0.085$  eV. Upper panel (a) – “bare” FS in paramagnetic state in the absence of AFM fluctuations. Panel (b) – AFM phase with  $\Delta = 0.05$  eV. Panel (c) – pseudogap state with  $\xi = 10a$  and  $\Delta = 0.05$  eV.